

Targeting the actin cytoskeleton: selective antitumor action via trapping PKC ϵ

F Foerster¹, S Braig¹, C Moser¹, R Kubisch¹, J Busse², E Wagner², E Schmoedel³, D Mayr³, S Schmitt⁴, S Huettel³, H Zischka⁴, R Mueller⁵ and AM Vollmar^{*1}

Targeting the actin cytoskeleton (CSK) of cancer cells offers a valuable strategy in cancer therapy. There are a number of natural compounds that interfere with the actin CSK, but the mode of their cytotoxic action and, moreover, their tumor-specific mechanisms are quite elusive. We used the myxobacterial compound Chondramide as a tool to first elucidate the mechanisms of cytotoxicity of actin targeting in breast cancer cells (MCF7, MDA-MB-231). Chondramide inhibits cellular actin filament dynamics shown by a fluorescence-based analysis (fluorescence recovery after photobleaching (FRAP)) and leads to apoptosis characterized by phosphatidylserine exposure, release of cytochrome C from mitochondria and finally activation of caspases. Chondramide enhances the occurrence of mitochondrial permeability transition (MPT) by affecting known MPT modulators: Hexokinase II bound to the voltage-dependent anion channel (VDAC) translocated from the outer mitochondrial membrane to the cytosol and the proapoptotic protein Bad were recruited to the mitochondria. Importantly, protein kinase C- ϵ (PKC ϵ), a prosurvival kinase possessing an actin-binding site and known to regulate the hexokinase/VDAC interaction as well as Bad phosphorylation was identified as the link between actin CSK and apoptosis induction. PKC ϵ , which was found overexpressed in breast cancer cells, accumulated in actin bundles induced by Chondramide and lost its activity. Our second goal was to characterize the potential tumor-specific action of actin-binding agents. As the nontumor breast epithelial cell line MCF-10A in fact shows resistance to Chondramide-induced apoptosis and notably express low level of PKC ϵ , we suggest that trapping PKC ϵ via Chondramide-induced actin hyperpolymerization displays tumor cell specificity. Our work provides a link between targeting the ubiquitously occurring actin CSK and selective inhibition of pro-tumorigenic PKC ϵ , thus setting the stage for actin-stabilizing agents as innovative cancer drugs. This is moreover supported by the *in vivo* efficacy of Chondramide triggered by abrogation of PKC ϵ signaling shown in a xenograft breast cancer model.

Cell Death and Disease (2014) 5, e1398; doi:10.1038/cddis.2014.363; published online 28 August 2014

The actin cytoskeleton (CSK) plays a crucial role in intracellular transport processes, migration of cells and cytokinesis. These processes require a highly dynamic behavior of the actin CSK that involves polymerization and depolymerization of actin filaments. Monomeric actin (G-actin) polymerizes in a head-to-tail manner to form helical actin filaments (F-actin) and the equilibrium between G-actin and F-actin is tightly regulated by so-called actin-binding proteins.¹ Besides being pivotal for cell motility and division, there is some evidence that actin CSK is also involved in cell death induction, but the underlying mechanisms and signaling molecules are not identified in detail.¹

One interesting candidate linking the actin CSK and cell death is protein kinase C- ϵ (PKC ϵ), a serine–threonine kinase of the PKC family² known to contain an actin-binding site.³ PKC ϵ is distributed in several tissues like heart and brain,^{4,5} and it is also overexpressed in a broad range of tumor malignancies like breast, stomach and gliomas.^{6–8} Because

of its distinct functions in proliferation and prosurvival signaling processes, PKC ϵ is an established oncoprotein and a promising target for anticancer therapy.^{9,10} In this context, PKC ϵ affects targets that regulate cell survival such as the transcription factors NF- κ B and Stat3 or the Bcl-2 protein Bad (Bcl2-associated death promoter).^{9–12} Bad is a proapoptotic BH3-only protein from the Bcl2-like gene family that is inactive when phosphorylated (Ser112) by kinases such as PKC ϵ .¹³ Moreover, PKC ϵ controls the linkage between the glycolytic enzyme Hexokinase II (HKII) and the voltage-dependent anion channel (VDAC) in mitochondria that is thought to be specific for tumor cells.^{12,14} VDAC, a channel located in the outer mitochondrial membrane facilitating the transport of small molecules, and hexokinase II, phosphorylating glucose as a rate-limiting step in glycolysis,¹⁵ are both discussed for their roles in malignancy.^{15,16}

Importantly, not only VDAC/HKII interaction but also Bad contribute to the regulation of the mitochondrial permeability

¹Department of Pharmacy, Pharmaceutical Biology, University of Munich, Munich, Germany; ²Department of Pharmacy, Pharmaceutical Biotechnology, University of Munich, Munich, Germany; ³Institute of Pathology, University of Munich, Munich, Germany; ⁴Institute for Molecular Toxicology and Pharmacology, Helmholtz Centre Munich, German Research Center for Environmental Health, Neuherberg, Germany and ⁵Helmholtz Institute for Pharmaceutical Research Saarland, Helmholtz Centre for Infection Research and Department of Pharmaceutical Biotechnology, Saarland University, Saarbrücken, Germany

*Corresponding author: AM Vollmar, Department of Pharmacy—Center for Drug Research, Pharmaceutical Biology, University of Munich, Butenandtstrasse 5-13, Munich 81377, Germany. Tel: +49 89 2180 77172; Fax: +49 89 2180 77170; E-mail: Angelika.Vollmar@cup.uni-muenchen.de

Abbreviations: ChA, Chondramide A; CSK, cytoskeleton; DMSO, dimethylsulfoxide; FRAP, fluorescence recovery after photobleaching; FCS, fetal calf serum; GFP, green fluorescent protein; HkII, Hexokinase II; MPT, mitochondrial permeability transition; PARP, poly(ADP-ribose) polymerase; PMA, phorbol-13-myristate-12-acetate; PKC ϵ , protein kinase C- ϵ ; ROI, region of interest; VDAC, voltage-dependent anion channel

Received 25.2.14; revised 14.7.14; accepted 16.7.14; Edited by J Chipuk

transition (MPT).^{14,17,18} This cell death eliciting process is initiated by an increased permeability of the mitochondrial inner membrane causing a depletion of the mitochondrial membrane potential, a net water influx into the mitochondrial matrix ('swelling') and finally the distension and rupture of the outer membrane.^{19–23} The outer membrane damage leads to the release of cytochrome *C* from the intermembrane space of mitochondria into the cytosol, activation of the initiator caspase 9 and finally to the induction of apoptosis.²⁴ Although several molecular aspects of the MPT are still under debate, several modulators of this process are known, for example, cyclosporin A as the 'proto-type' inhibitor of calcium-induced MPT.^{25,26}

Roy *et al.*¹⁷ showed that the dephosphorylated, active form of Bad leads to MPT, and also that VDAC is thought to participate in this process.¹⁶ HkII binding to VDAC, on the other hand, stabilizes VDAC and prevents MPT and apoptosis.¹⁴ Thus, disrupting the VDAC/HkII complex as well as activation of Bad could be attractive strategies to selectively kill tumor cells via the MPT. In this work we aimed to characterize and understand the molecular link between actin CSK and induction of apoptotic processes. To this end we hypothesized that PKC ϵ possessing an actin-binding site could be a signaling molecule bridging actin CSK and cell death. We used Chondramide A (ChA), a myxobacterial cyclodepsipeptide isolated from *Chondromyces crocatus* that is²⁷ known to induce polymerization of actin,^{27,28} as a chemical tool to potentially affect PKC ϵ -mediated cell death induction. Chondramide has been shown to inhibit cancer cell proliferation,^{28,29} but closer mechanistic insights are not available.

In fact, our study shows that overpolymerization of actin CSK via Chondramide leads to inhibition of a tumor-specific PKC ϵ signaling pathway, resulting in the induction of MPT and apoptosis *in vitro* as well as in a xenograft breast cancer mouse model *in vivo*. These data uncover the potential of actin-binding drugs in cancer therapy.

Results

Chondramide inhibits actin dynamics and induces apoptosis via the intrinsic pathway. The dynamics of globular and filamentous actin equilibrium have been analyzed using the fluorescence recovery after photobleaching (FRAP) technique: a distinct region of MCF7 mammary cancer cells transfected with green fluorescent protein (GFP)-tagged β -actin has been bleached by laser (488 nm) and the actin filament dynamics were observed by time lapse microscopy (Figure 1b). Untreated cells recover from photobleaching within seconds seen by the rapid disappearance of the bleached area (Figure 1b upper panel, white arrows). In contrast, cells treated with 300 nM ChA (Figure 1a) for 30 min display a massive reduction of the mobile, globular actin fraction (Figure 1b lower panel, white arrows). Quantification of fluorescence recovery confirms a distinct abrogation of actin filament dynamics by ChA (Figure 1b, graph). Finally, ChA treatment time dependently induces agglomeration of globular actin that results in formation of actin lumps, as shown in Figure 1c.

Besides affecting the actin CSK, ChA treatment (300 nM, 48 h) induces apoptosis in both MCF7 and MDA-MB-231 mammary cancer cells. Cell death was quantified using an Annexin V/PI co-staining assay (Figure 2a). ChA treatment (300 nM, 24 h) leads to a depletion of mitochondrial membrane potential ($\Delta\Psi_m$) analyzed by the use of the mitochondrial selective dye JC-1 (Figure 2b). Fluorescence profiles of both cell lines show a shift toward green fluorescence of JC-1 (shift to the left) after ChA treatment, indicating a decrease in mitochondrial membrane potential. In line with disruption of mitochondrial membrane potential, ChA treatment (300 nM) results in a release of cytochrome *C* from the mitochondria in both cell lines. Figure 2c shows FACS analysis of cytochrome *C* remaining in the mitochondria of cells treated with ChA for 24 h compared with untreated cells. Accordingly, downstream signaling of cytochrome *C* release, namely activation of caspases, was evaluated. Western blot analysis shows a decrease of pro-caspase 9 and the cleavage of poly(ADP-ribose) polymerase (PARP), a well-known substrate of effector caspases, in cells treated with 300 nM ChA (24 h) (Figure 2d). In sum, Figure 2 demonstrates that ChA induces cell death via the intrinsic apoptosis pathway.

Chondramide induces translocation of HkII from mitochondria and dephosphorylation of Bad pointing to a role of the MPT. As ChA depleted $\Delta\Psi_m$ and induced mitochondrial cytochrome *C* release in mammary cancer cells, both hallmarks of the MPT, we focused on major players involved in this process. VDAC, which is localized at the outer mitochondrial membrane, interacts with HkII, thereby negatively modulating MPT and preventing apoptosis.¹⁵ We found that the binding of HkII and VDAC is impaired by ChA (Figure 3a). HkII colocalizes with mitochondria shown as a distinct dot-like pattern in control cells. In contrast, cells treated with 300 nM ChA displayed a rather diffuse localization of HkII, suggesting a disruption of the mitochondrial VDAC/HkII interaction. Western blot experiments support this notion as decreased protein levels of HkII were found in the mitochondrial fraction of cells treated with ChA (300 nM, 6 and 24 h) (Figure 3b).

Moreover, ChA affects a further regulator of the MPT, that is, the Bcl-2 protein Bad.¹⁷ Protein level of Ser-112 phosphorylated, inactive Bad decreased dose dependently after treatment of cells with ChA (100 and 300 nM, 6 h) with constant total Bad protein levels (Figure 3c). Consequently, in cells treated with ChA an intensified colocalization of Bad with mitochondria was observed in comparison with untreated cells (Figure 3d), supporting the idea that proapoptotic, mitochondrial Bad is increased by chondramide because of abrogation of the inactive, phosphorylated form of Bad.

Finally, the involvement of the MPT in ChA-induced cell death was further supported by a set of experiments using isolated mitochondria of untreated and ChA-treated MDA-MB-231 cells. In mitochondria isolated from untreated and ChA-treated cells, MPT could be induced by 400 μ M Ca²⁺ (data not shown). Importantly, cyclosporin A efficiently blocked the Ca²⁺-induced loss of $\Delta\Psi_m$ (Supplementary Figure 1A) and confirms participation of the MPT in isolated mitochondria from control cells (Supplementary Figure 1B). In contrast, isolated mitochondria from ChA-treated cells only weakly

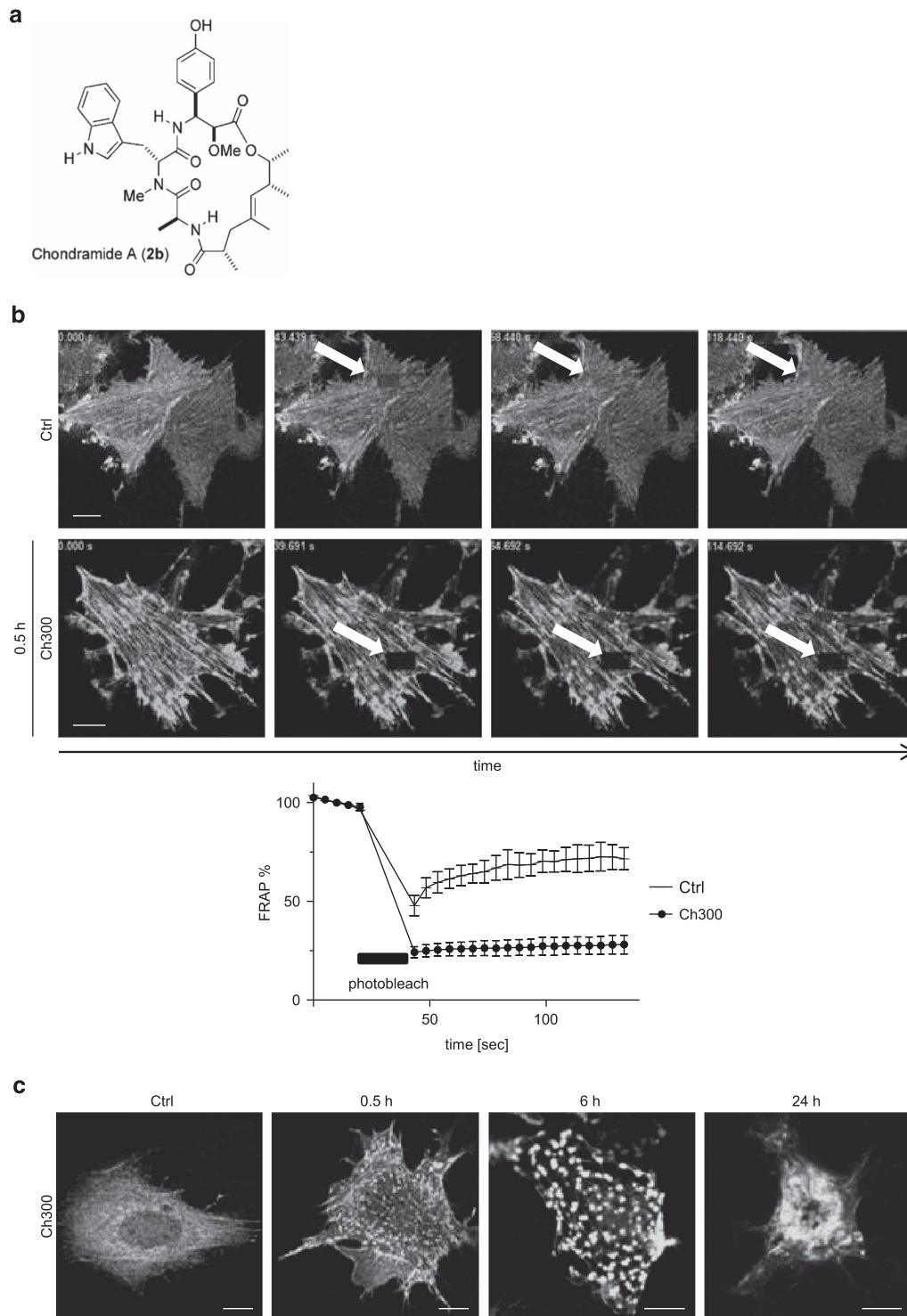


Figure 1 Chondramide A (ChA) inhibits actin dynamics and leads to agglomeration of actin. **(a)** Molecular structure of ChA. **(b)** MCF7 cells were transfected with mGFP- β -actin and treated with 300 nM ChA for 30 min. The mobile actin fraction was quantified by FRAP analysis. (Upper panel) White arrows indicate the photobleached area in representative images (Ctrl, untreated cells; Ch300, cells treated with 300 nM ChA). (Lower panel) Values represent the % fluorescence recovery over time of mGFP- β -actin after photobleach. **(c)** Time course of actin hyperpolymerization of MCF7 cells expressing mGFP- β -actin and treated with 300 nM ChA (Ch300) for 0.5, 6 and 24 h. Scale bar indicates 10 μ m. Each experiment was independently performed three times

responded toward the inhibitory action of cyclosporin A. A progressing depletion of $\Delta\Psi$ m coincided with an increasing extent of mitochondria that have undergone swelling (i.e., MPT) (Supplementary Figure 1A and 1B).

Thus, by altering known modulators of the MPT, ChA leads to a release of cytochrome C from mitochondria. The MPT-blocking HklI/VDAC interaction is disrupted, Bad localizes to mitochondria and cyclosporin A inhibition of the MPT is

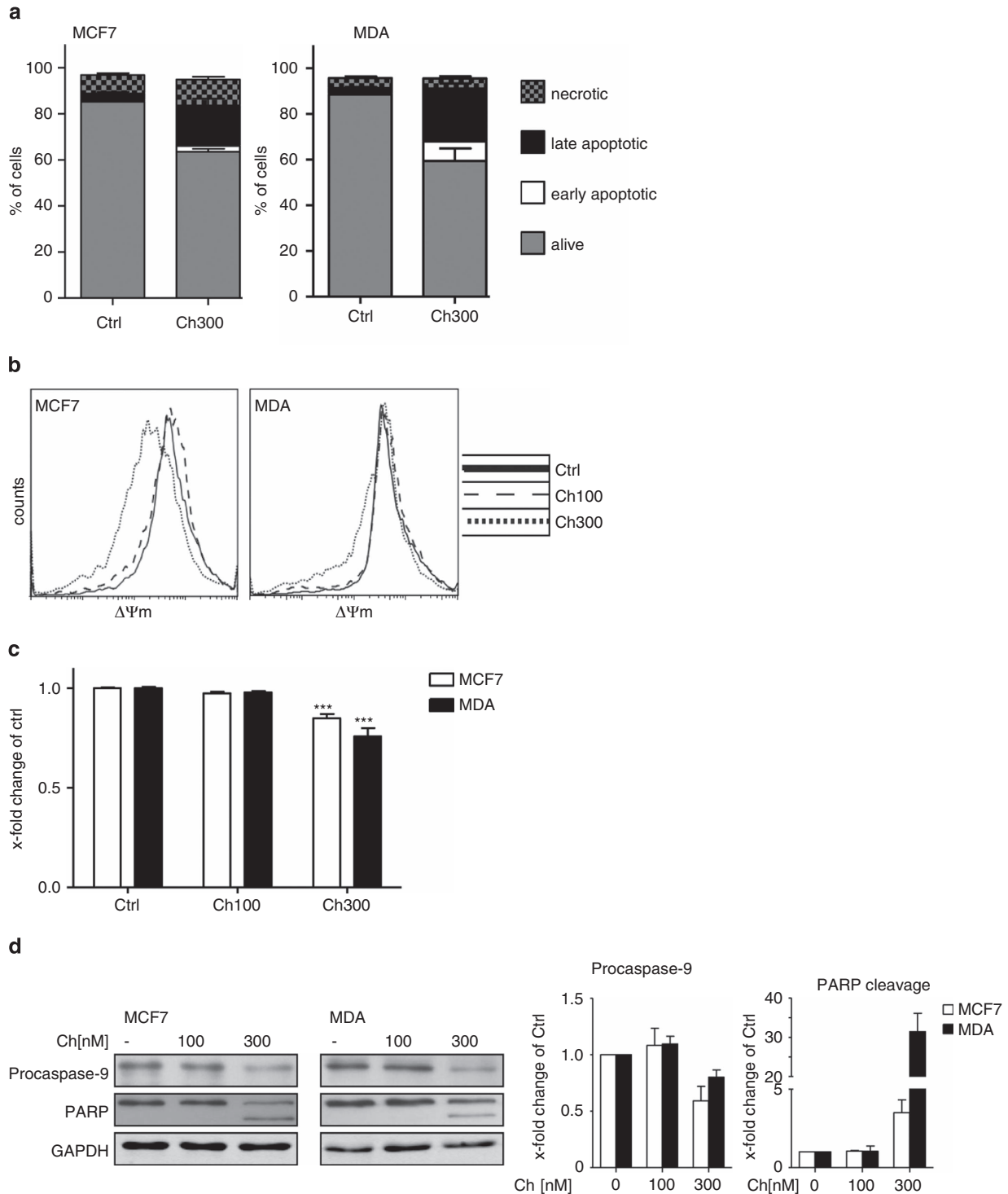


Figure 2 Chondramide A (ChA) induces apoptosis in breast cancer cell lines via the intrinsic mitochondrial pathway. **(a)** MCF-7 as well as MDA-MB-231 cells were treated with ChA (300 nM, 48 h) and analyzed for apoptotic cell death by staining with Annexin-V-FITC/PI. Living cells are marked in gray, early apoptotic cells in white (Annexin V positive), late apoptotic cells in black (Annexin V and PI positive) and necrotic cells in spotted gray (PI positive). **(b)** Mitochondrial membrane potential ($\Delta\Psi_m$) of cells was determined by flow cytometry using JC-1 as mitochondrial selective dye. MCF7 and MDA-MB-231 cells were treated with 100 and 300 nM ChA for 24 h. **(c)** Mitochondrial cytochrome C content in cells (MCF7, MDA-MB-231) treated for 24 h with ChA (100 nM, 300 nM) was measured via flow cytometry. **(d)** Western blot analysis of procaspase-9 and cleavage of PARP as parameters for activation of caspase-9 and effector caspases, respectively, was performed using cells exposed to ChA (100 and 300 nM, 24 h). The graphs represent the quantitative analysis of the band intensities of Pro-caspase 9 and the PARP cleavage product. Blotting for GAPDH serves as loading control. A representative blot out of three is shown. Bars represent the mean \pm S.E.M. of three independent experiments performed in triplicates, *** $P < 0.001$ (one-way ANOVA, Bonferroni)

abrogated, thus finally resulting in inhibition of cytochrome *C* release.

ChA inhibits PKC ϵ activation by trapping in actin bundles. Ser112-phosphorylation of Bad as well as the interaction of Hkll with VDAC are known to be regulated by PKC ϵ .¹⁷ As PKC ϵ contains an actin-binding site, our working hypothesis focused on PKC ϵ as a link between the effect of ChA on actin CSK and the induction of apoptosis via mitochondrial activation. As a first step to verify this idea, the postulated interaction of actin CSK and PKC ϵ was confirmed (Figure 4). Immunostaining of mGFP- β -actin-transfected MCF7 cells showed an enrichment of PKC ϵ in ChA-induced actin bundles at 6 and 24 h after treatment (Figure 4a). To control that we are not observing a compound-specific effect of ChA, two other actin-polymerizing agents (jasplakinolide and dolicolide) were used in this colocalization assay, and also here it could be shown that PKC ϵ is trapped in actin bundles induced by jasplakinolide and dolicolide (Supplementary Figure 2). Interestingly, PKC α , which does not contain an actin-binding site, shows no colocalization in ChA-induced actin lumps (Supplementary Figure 3). Analysis of cytosolic and cytoskeletal fractions of MDA-MB-231 (Figure 4b) and MCF7 cells (Supplementary Figure 4) showed increased actin content in the CSK fraction after ChA treatment compared with control cells that, importantly, is accompanied by enhanced PKC ϵ protein levels, but not PKC α . GAPDH in the cytoskeletal fraction serves as impurity control for cytoplasmic contaminants. These data point to a specific interaction between actin CSK and PKC ϵ and its modulation via ChA treatment. In fact, ChA affects activation of PKC ϵ , as shown in Figure 4c. As translocation of PKCs to the cell membrane is a typical hallmark for their activation, MDA-MB-321 cells were stained for PKC ϵ after exposure to phorbol-13-myristate-12-acetate (PMA), a common inducer of PKCs (1 μ M, 30 min). PMA-stimulated cells clearly display PKC ϵ protein localized on the cellular membrane, whereas treatment with ChA results in a significant decrease of PKC ϵ at the plasma membrane quantified by counting the respective cells (Figure 4c). Taken together, Figure 4 displays a trapping of PKC ϵ and impaired PKC ϵ activation as consequence of ChA-induced polymerization of actin CSK.

ChA-induced cell death is dependent on PKC ϵ expression. In order to prove the link between PKC ϵ and ChA-induced apoptosis, cells overexpressing PKC ϵ were analyzed for their apoptotic response upon ChA treatment (Figure 5a). Overexpression of PKC ϵ was verified by western blot analysis (insets; Figure 5a) and does not affect itself cell viability (data not shown). PKC ϵ -transfected MCF7 and MDA-MB-231 cells show a significant decrease in sensitivity toward ChA treatment compared with cells transfected with empty vector plasmid, thus verifying the importance of PKC ϵ in cell death induction mediated by Chondramide. This was further support by siRNA experiments in MDA-MB-231. Down-regulation of PKC ϵ resulted in an increased rate of Annexin V-positive cells, indicating the induction of apoptosis by PKC ϵ silencing (Supplementary Figure 5).

ChA treatment displays tumor cell specificity. The distinct role of PKC ϵ in ChA-induced cancer cell apoptosis and even more its selectivity toward tumor cells was demonstrated by another set of experiments: the effect of ChA on the two tumor cell lines (MCF-7, MDA-MB-231) was compared with that on the nontumorigenic breast epithelial cell line MCF10-A (Figure 5b). Treatment with 300 nM ChA disrupts actin CSK in MCF10-A as well (Supplementary Figure 6); however, MCF10-A cells show no increased cell death rate in contrast to MCF7 and MDA-MB-231 cells (Figure 5b). To link PKC ϵ to induction of apoptosis, we compared PKC ϵ protein levels in all three cell lines. Of note, MCF10-A nontumorigenic cells express much less PKC ϵ protein than MCF7 and MDA-MB-231 cancer cells (Figure 5c). A similar picture was observed when analyzing breast tissue from patients. Human breast cancer tissues display a massive expression of PKC ϵ , whereas healthy breast tissues show only weak staining for PKC ϵ besides in the acini of breast glandular cells (Figure 5d). In sum, ChA-induced apoptosis is mediated by actin CSK disruption and is highly depending on the expression of PKC ϵ in cells.

Chondramide reduces tumor growth and induces actin polymerization, PKC ϵ trapping and apoptosis *in vivo*. Using a MDA-MB-231 xenograft mouse model administration of 0.75 mg/kg, Chondramide was shown to significantly reduce tumor growth as monitored by tumor volume (Figure 6a). Tumor tissue was examined for apoptotic cells (TUNEL assay) and showed a significant increase of apoptotic nuclei in the Chondramide-treated group compared with control tissue (Figure 6b). Furthermore, we analyzed actin CSK and PKC ϵ in cryosections of tumor tissue. Chondramide also leads *in vivo* to a disruption of actin CSK (especially on the border of tumors) and, moreover, PKC ϵ is localized in actin bundles in Chondramide-treated tumors (Figure 6c). In sum, this set of experiments confirms Chondramides' cell death-inducing mechanism *in vivo*. The cartoon in Figure 6d summarizes the postulated molecular mechanism of Chondramide's mode of action.

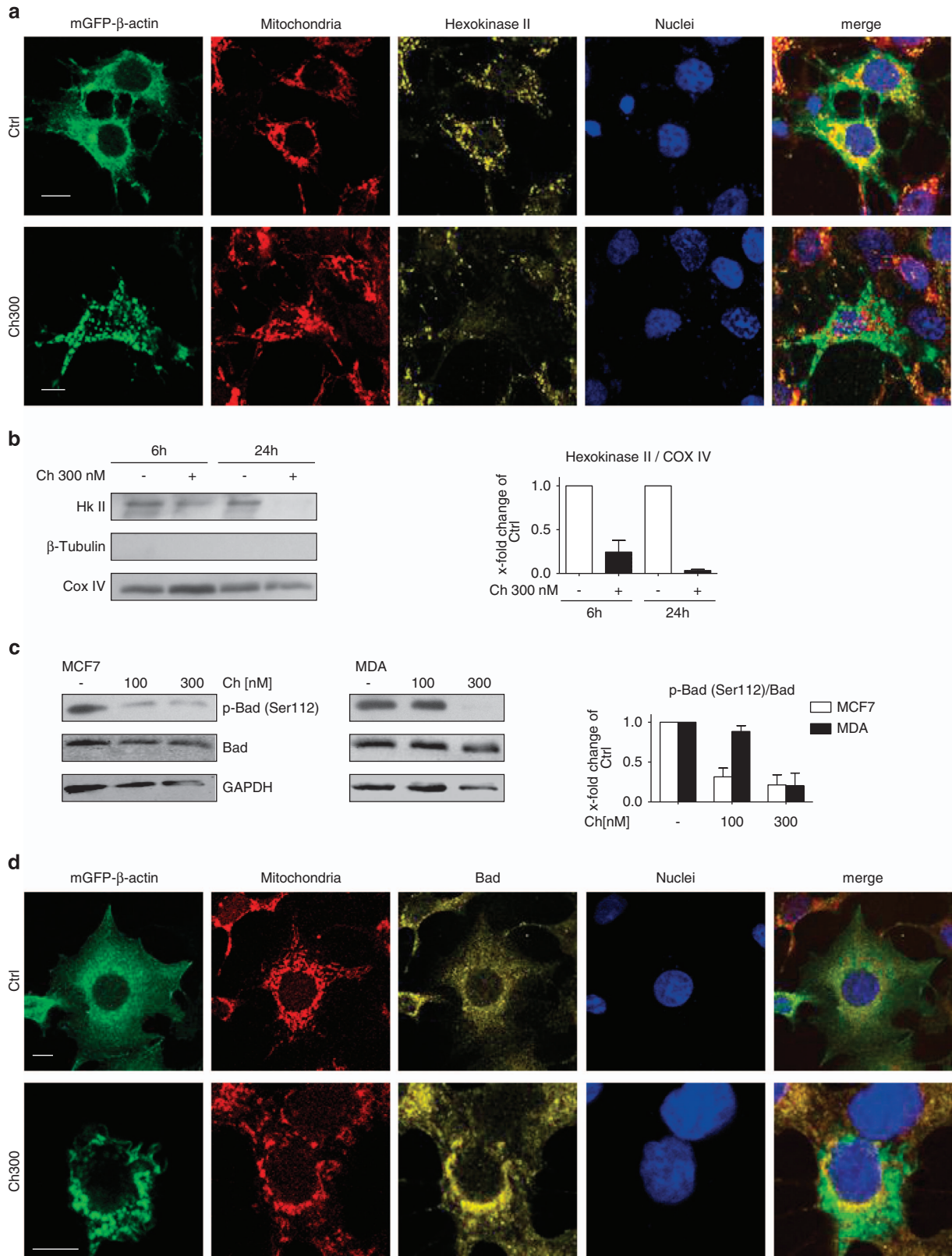
Discussion

The actin and microtubule cytoskeletons play pivotal roles in cancer biology as they regulate tumor relevant processes, for example, cell cycle, morphogenesis or migration.³⁰ Whereas drugs such as vinca alkaloids or taxanes that target microtubules are well established in the clinic,³¹ compounds binding to the actin CSK are still far away from their therapeutical application. One reason might be lack of knowledge on their tumor-specific mechanism of action.

The data communicated here provide a conceptual framework for actin-polymerizing agents such as Chondramide as tumor cell-specific cytotoxic drugs. The major findings were as follows. (1) The actin CSK is involved in specific apoptotic signaling via PKC ϵ and regulation of MPT. As PKC ϵ is overexpressed in tumor cells, a tumor cell-selective mode of action is proposed. (2) Actin-targeting Chondramide masters the challenge of isoform-specific inhibition of PKC, namely protumorigenic PKC ϵ . (3) Chondramide induces apoptosis and displays *in vivo* efficacy via disruption of PKC ϵ signaling.

Pharmacological interruption of actin dynamics has been reported before to lead to cell death, but the exact mechanisms remain unclear.¹ Posey *et al.*³² hypothesized a role of

gelsolin, an actin-binding protein, for apoptosis induced by another actin-polymerizing natural compound named jasplakinolide; however, gelsolin overexpression was shown to



have no impact on apoptosis induction by jasplakinolide. We used Chondramide as a chemical tool to learn more about actin-specific apoptotic signaling. Chondramide, similar to jasplakinolide,³³ hyperpolymerizes the actin cytoskeleton, induces agglomeration of actin that assembles over time and forms massive amorphous actin bundles that contain actin-binding proteins as reported previously.³⁴ Our driving strategy was to search for regulators of cell death containing an actin-binding site and to examine whether they might be trapped within these actin structures and thereby display decreased functionality. We came up with PKC ϵ , a member of the PKC family, that, on one hand, possesses an actin-binding motif^{3,5} and is, on the other hand, a crucial regulator of several pro-survival pathways.^{6–11}

The PKC family has been an exciting target for drug discovery especially in cancer ever as they were identified as intracellular receptors for the tumor-promoting agents phorbol esters.³⁵ However, major challenges such as dissecting the contribution of PKC isozymes to cancer progression or developing modulators specific for the PKC isozymes are still to be met. PKCs are either pro-mitogenic or inhibit cell cycle progression depending on isozyme and cell type. PKC α and PKC Δ , for instance, promote anti-mitotic responses³⁶ in tumor cells, whereas PKC ϵ is required for cancer cell survival.^{10,11} Furthermore, PKC ϵ has been shown to be overexpressed in various types of cancer including breast cancer,^{6,9} supported by our own data. PKC ϵ mediates oncogenic activities as it affects the activity of transcription factors like ATF2, NF- κ B and Stat3,^{12,37,38} and also addresses distinct targets in the apoptotic machinery of cells such as the BH3-only Bcl2-family protein Bad. Bad exerts its pro-apoptotic functions in a dephosphorylated form and PKC ϵ is known to directly phosphorylate Bad on serine 112, thus inhibiting the pro-apoptotic activity of Bad^{17,39,40} by preventing MPT¹⁷ and hence the onset of apoptosis. PKC ϵ counteracts the MPT not only via inactivation of Bad but also by maintaining the complex of VDAC and HklI at the outer mitochondrial membrane. Phosphorylation of VDAC⁴ as well as phosphorylation of the transcription factor ATF2, which then attenuates apoptosis through saving the VDAC/Hk interaction,³⁷ are discussed as mechanisms for the pro-survival features of PKC ϵ . The association between the glycolytic enzyme HklI and VDAC has been reported to be specific for cancer cell mitochondria and thus its disruption promises tumor cell-specific apoptosis.¹⁴ Inhibition of PKC ϵ leads to MPT because of loss of VDAC/Hk complex as well as loss of inactivated Bad, both of which could be clearly demonstrated for Chondramide treatment. Our work provides evidence for MPT as target in apoptosis induction by PKC ϵ inhibition in Chondramide-treated cells. Supplementary Data show that cyclosporin A, which normally blocks the Ca²⁺-induced MPT, is not able to

prevent mitochondrial swelling (i.e., the MPT) in isolated mitochondria from cells treated with Chondramide, thus further supporting the involvement of MPT. Moreover, our data offer an explanation of how changes in actin CSK dynamics lead to cell death and proposes actin CSK as a specific antitumor target.

As mentioned above, identification of isozyme-selective modulators of PKCs has been a major challenge taken up by various approaches such as the development of ATP-competitive small-molecule inhibitors that bind to the catalytic domain of the kinase, phorbol ester derivatives that mimic the binding of diacylglycerol or peptides that prevent the anchoring of the PKC to its RACK (receptor of activated C-kinase) that brings the activated enzyme to its substrate.³⁵ Our data propose Chondramide as an indirect PKC ϵ -specific inhibitor based on the fact that particularly PKC ϵ because of its actin-binding site is trapped by Chondramide-induced actin polymerization. The role of PKC ϵ as a promising tumor-specific therapeutic target and as a major player in Chondramide-induced tumor cell death is supported by two facts. First, nontumor cells (MCF-10A breast epithelial cells) show low level of PKC ϵ and are not sensitive to Chondramide. Second, PKC ϵ overexpression, leading to free PKC ϵ that is not trapped in actin bundles, rescues Chondramide-induced apoptosis.

Importantly, Chondramide shows *in vivo* efficacy. Treatment of mice bearing a xenograft breast tumor (MDA-MB-231 cells) with Chondramide leads to reduction of tumor growth by inducing apoptosis through PKC ϵ trapping in actin bundles.

Our data link actin, a target distributed in all eukaryotic cells, to the cancer-specific protein PKC ϵ and open new therapeutic approaches by using actin-overpolymerizing compounds. Thus, our work encourages comprehensive pharmacological evaluation of this class of actin-targeting agents in tumor therapy.

Materials and Methods

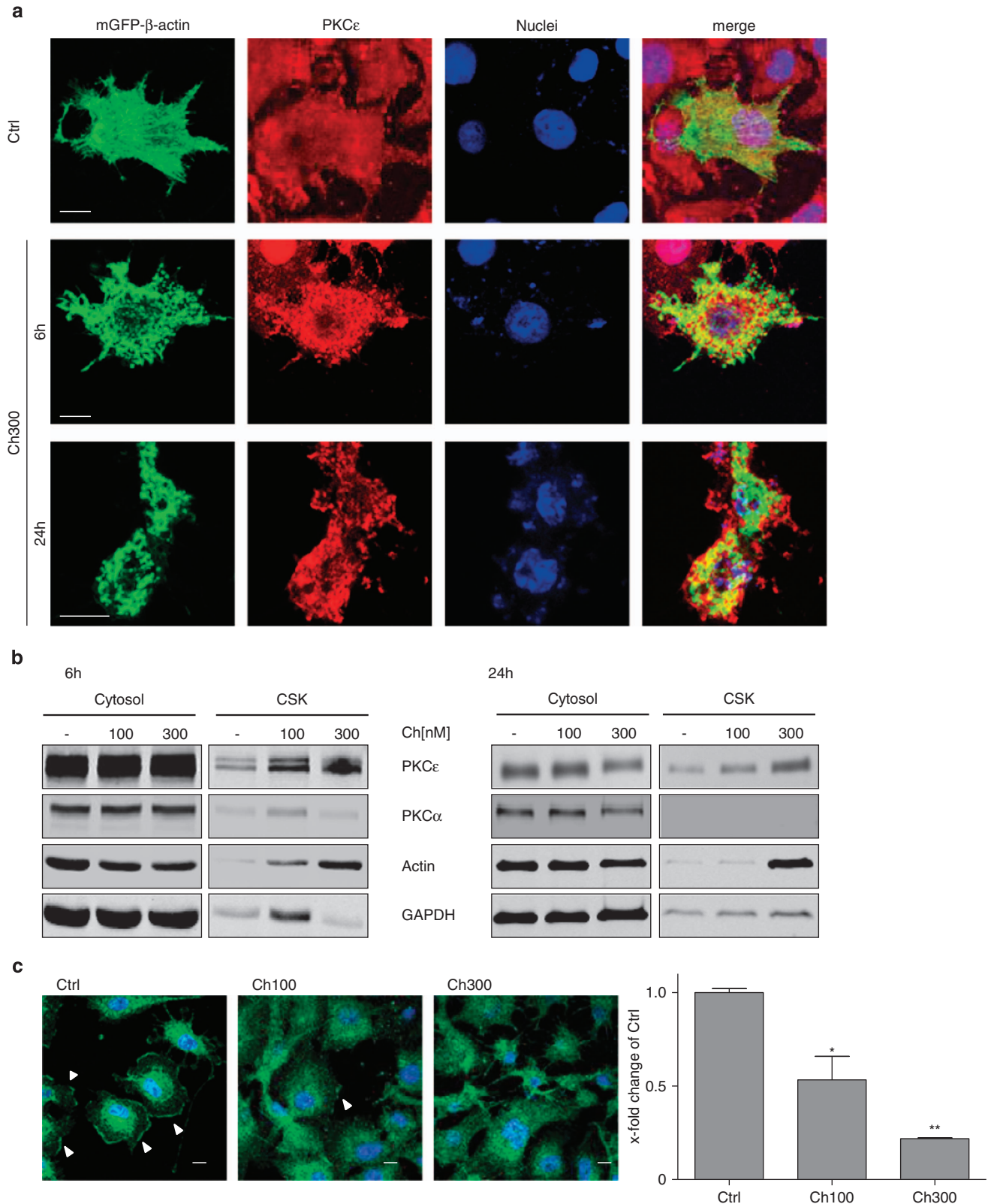
Reagents. Chondramide A (chemical structure Supplementary Figure 1) was isolated as described previously²⁹ and dissolved in dimethylsulfoxide (DMSO). The PKC activator PMA was purchased from Merck Millipore (Darmstadt, Germany) and dissolved in DMSO. Jasplakinolide was purchased from Sigma-Aldrich (Taufkirchen, Germany) and Dolicolide was a gift from Professor Karl-Heinz Altmann (ETH Zurich, Zurich, Switzerland).

Cell culture. The human epithelial breast cancer cell line MCF7 was purchased from the DSMZ (Braunschweig, Germany) and maintained in RPMI-1640 medium supplemented with 10% heat-inactivated fetal calf serum (FCS, Biochrom AG, Berlin, Germany), 1% pyruvate (Sigma-Aldrich), 125 μ g/l insulin (Sigma-Aldrich), 1% nonessential amino acids (PAA, Pasching, Austria) and 1% penicillin/streptomycin (Sigma-Aldrich) at 37°C and 5% CO₂. MCF10-A nontumorigenic epithelial cells were from ATCC (Manassas, VA, USA) and cultivated in RPMI-1640 medium supplemented with 5% horse serum (PAA), Insulin 125 μ g/l (Sigma-Aldrich), EGF 100 ng/ml (PeproTech, Hamburg, Germany), hydrocortisone 0.8 μ g/ml (Sigma-Aldrich), cholera toxin 0.16 μ g/ml (Sigma-Aldrich)

Figure 3 Treatment with Chondramide A (ChA) leads to the dislocation of Hexokinase II (HklI) from mitochondria and activation of pro-apoptotic Bad. (a) MCF-7 cells transfected with mGFP- β -actin were treated with 300 nM ChA for 6 h, fixed and co-stained with Mitotracker red CMX-ROS and anti-Hexokinase II antibody followed by confocal microscopic analysis. Scale bar indicates 10 μ m. Representative images are shown. (b) Western blot of HklI in mitochondrial fraction of MDA-MB-231 cells treated with 300 nM ChA for 6 and 24 h. Cytosolic and mitochondrial fractions were separated. Immunoblotting for β -tubulin and COX IV were used for controlling purity of mitochondrial fraction and loading control, respectively. Representative blot of the mitochondrial fraction and the respective quantification is shown. (c) Western blot analysis for Bad and phospho-(Ser112)-Bad in MCF7 and MDA-MB-231 cells treated with 100 and 300 nM ChA for 6 h and quantitative analysis of band intensities. (d) MCF7 cells transfected with mGFP- β -actin were treated with 300 nM ChA for 6 h, fixed and co-stained with Mitotracker red CMX-ROS and anti-Bad-antibody followed by confocal microscopic analysis. Scale bar indicates 10 μ m. Representative images are shown. Each experiment was performed independently three times

and 1% penicillin/streptomycin. MDA-MB-231 was purchased from cell lines service (Eppelheim, Germany) and maintained in DMEM high glucose (PAA) supplemented with 10% FCS and 1% penicillin/streptomycin.

Transfection of mGFP- β -actin in MCF7. MCF7 cells were transfected with pCAG-mGFP- β -actin using the FuGene transfection kit from Promega (Mannheim, Germany) according to manufacturer's



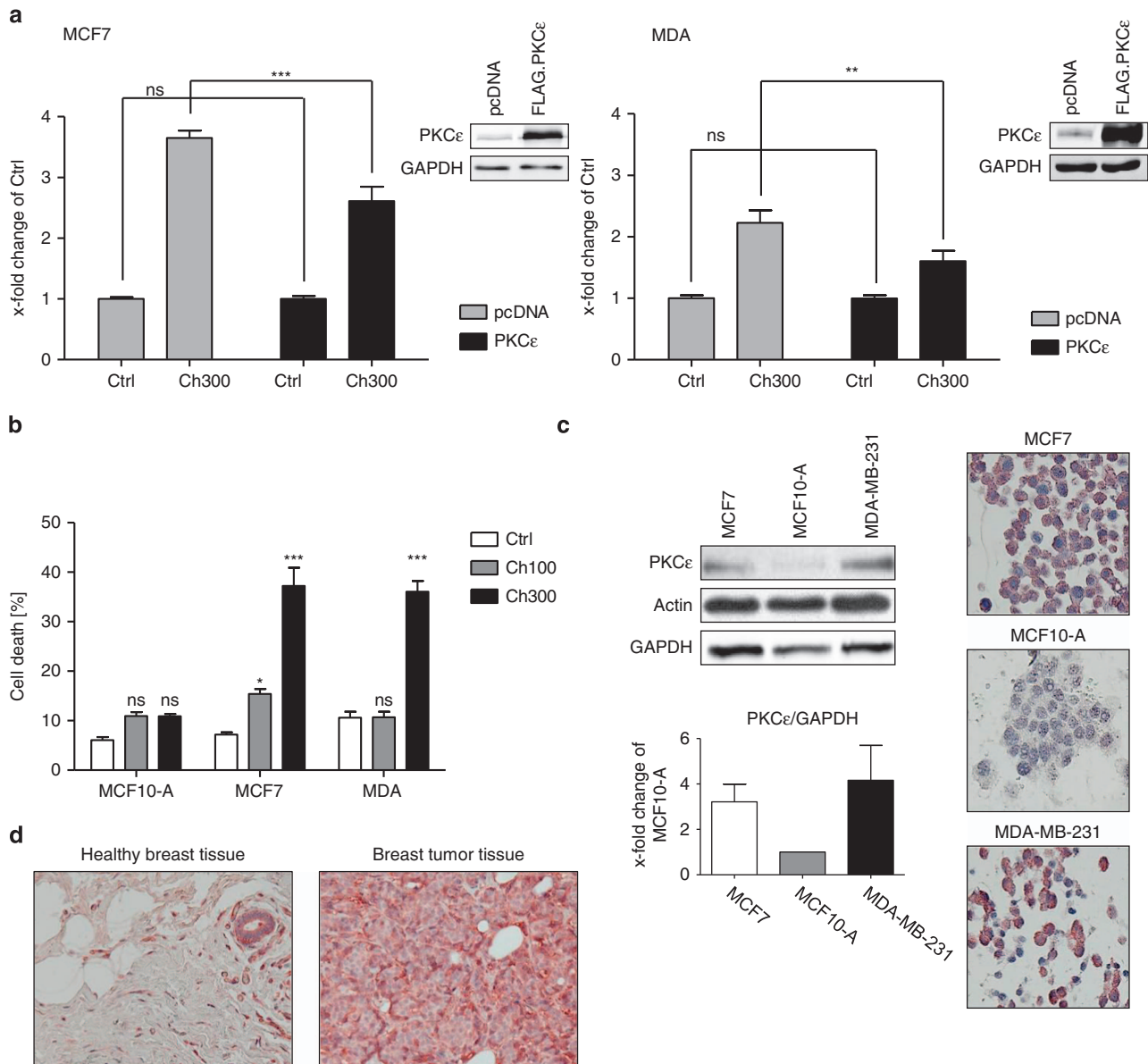
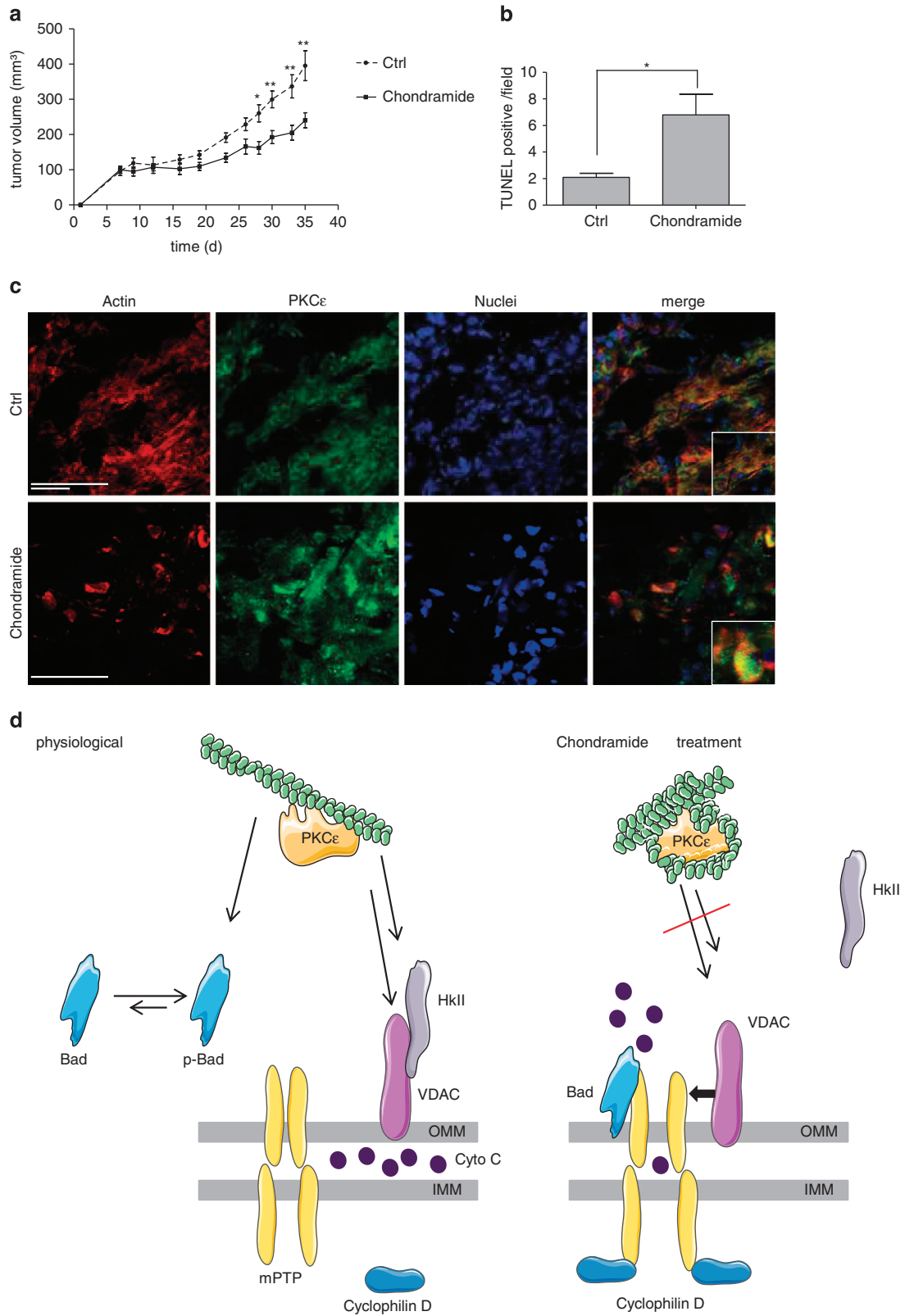


Figure 5 PKC ϵ overexpression rescues cells from Chondramide A (ChA)-induced apoptosis and noncancerous cells are less susceptible to ChA. (a) MCF7 and MDA-MB-231 cells were transfected with FLAG.PKC ϵ or an empty vector and treated with 300 nM ChA for 24 h. The number of dead cells was analyzed using the propidium iodide (PI) exclusion assay for MCF7 cells and Annexin V staining for MDA-MB-231 cells. Overexpression of PKC ϵ was confirmed by western blot (insets). The graphs show the results normalized to the according control. Each experiment was independently performed three times. (b) The adenocarcinoma cell lines MCF7, MDA-MB-231 and the nontumorigenic epithelial breast cell line MCF10-A were evaluated for their responsiveness to ChA by monitoring PI-positive cells after 24 h. (c) Comparison of PKC ϵ levels is shown in MCF7, MDA-MB-231 and MCF10-A via western blot (graph shows quantification) as well as via immunohistochemistry. GAPDH and actin serve as loading control. Each experiment was independently performed three times. (d) Representative PKC ϵ tissue stainings of healthy breast tissue and mammary tumor tissue. Nuclei are counterstained with hematoxylin. Bars represent the mean \pm S.E.M. of three independent experiments performed in triplicates, * P < 0.05, ** P < 0.01, *** P < 0.001 (one-way ANOVA, Bonferroni)

Figure 4 PKC ϵ colocalizes with Chondramide A (ChA)-induced actin bundles, accumulates in the cytoskeletal fraction (CSK) and shows decreased activity upon ChA treatment. (a) MCF7 cells were transfected with mGFP- β -actin and incubated with 300 nM ChA for 6 and 24 h. Cells were fixed and stained for PKC ϵ . Yellow color in merged images indicates colocalization of PKC ϵ with actin bundles. Nuclei were stained by Hoechst 33342. Scale bar indicates 10 μ m. (b) Cytosolic and cytoskeletal fractions of MDA-MB-231 cells were isolated, resolved by SDS-PAGE and immunoblotted using antibodies against PKC α , PKC ϵ , actin and GAPDH. (c) PKC ϵ activation was determined via monitoring the translocation to the plasma membrane. MDA-MB-231 cells treated with 100 and 300 nM ChA for 6 h were costimulated with PMA (1 μ M, 30 min), fixed and stained for PKC ϵ . Quantification of cells with activated PKC ϵ was done by analyzing at least 80 cells per group for their PKC ϵ membrane localization (confocal microscopy). Shown are representative images, and white arrows indicate cells with active PKC ϵ . Scale bar indicates 10 μ m. The graph shows a normalized statistical analysis. All experiments were performed independently three times. Bars represent the mean \pm S.E.M. of three independent experiments performed in triplicates, * P < 0.05, ** P < 0.01 (one-way ANOVA, Bonferroni)



instructions. pCAG-mGFP-actin was a gift of Ryohei Yasuda⁴¹ (Addgene plasmid 21949, Cambridge, MA, USA).

Fluorescence recovery after photobleaching. MCF7 cells transfected with mGFP- β -actin were seeded in ibidi- μ -slides (ibidi, Martinsried, Germany) and incubated in the climate chamber of a Zeiss LSM 510 (Zeiss, Jena, Germany) confocal microscope at 5% CO₂, 37°C. Regions of interest (ROIs) of equal size were chosen in untreated and ChA (300 nM, 0.5 h)-treated cells and were bleached by high laser energy (488 nm). Images were taken every 5 s, lasting for ~2.5 min and the fluorescence intensity within the ROI was measured. Cells were randomly chosen for bleaching and quantification of fluorescence recovery was done using the LSM image browser software (Zeiss).

Quantification of cell death. For analysis of membrane phosphatidylserine exposure, phosphatidylserine switch to the outer leaflet of the plasma membrane was analyzed by Annexin-V staining using the respective apoptosis detection kit (ebioscience, San Diego, CA, USA) according to the manufacturer's instructions. Cells were analyzed by a FACSCalibur cytometer (Becton Dickinson, Heidelberg, Germany).

For propidium iodide exclusion assay, cells were harvested, washed, exposed to a solution of propidium iodide (50 μ g/ml) (Sigma-Aldrich) in PBS and immediately analyzed by flow cytometry using a Becton Dickinson FACSCalibur.

Mitochondrial potential ($\Delta\Psi$ m). Cells were harvested and incubated with JC-1 (Alexis Biochemicals, Loerrach, Germany; 1.25 μ M, 37°C, 30 min). Mitochondria with an intact potential display JC-1 red fluorescing aggregates, whereas in mitochondria with disrupted potential JC-1 is monomeric and green fluorescent. The shift in fluorescence was monitored by a FACSCalibur cytometer (Becton Dickinson) using channel FL1-H for green fluorescence. Membrane potential and swelling of isolated mitochondria was assessed by Rh123 fluorescence quenching as described in literature.⁴²

Cytochrome C release. Analysis of cytochrome C release was performed as previously described.⁴³ Briefly, cells were incubated in a digitonin-containing buffer for 30 min on ice (0.2 mM Na-EGTA, 100 mM KCl, 50 μ g/ml digitonin, PBS), fixed with 4% PFA for 20 min and unspecific binding was blocked (3% BSA, 0.05% Saponine (Sigma-Aldrich), 1 h, RT) before incubation with cytochrome C antibody overnight at 4°C and staining with the secondary antibody for 1 h. Cytochrome C antibody was purchased from Cell Signaling Technology (Danvers, MA, USA) and secondary goat-anti-rabbit-Alexa-488 antibody was obtained from Invitrogen (Darmstadt, Germany). Fluorescence was detected using a FACSCalibur cytometer (Becton Dickinson). A decrease in fluorescence intensity indicates a loss of mitochondrial cytochrome C that is washed out after cell membrane permeabilization.

Western blot analysis. Cells were harvested, washed and lysed on ice with a buffer containing 2 mM EDTA, 137 mM NaCl, 10% glycerol, 2 mM Na₄P₂O₇, 20 mM Tris-base, 1% Triton-X 100, 20 mM sodiumglycerolphosphate, 10 mM NaF, 2 mM Na₃VO₄, 1 mM phenylmethylsulfonylfluoride and Complete protease inhibitor (Roche, Mannheim, Germany). Equal amounts of protein were separated using SDS-PAGE and blotted on nitrocellulose membranes (GE Healthcare, Munich, Germany). Membranes were probed with antibodies as indicated. Following antibodies were used: actin (Merck Millipore), Bad/phospho-Ser112-Bad, β -Tubulin, Caspase 9, COX IV, Hexokinase II, PARP (Cell Signaling Technology), GAPDH, PKC α , PKC ϵ (Santa Cruz Biotechnology, Dallas, TX, USA), goat-anti-mouse IRDye 800 cw (LI-COR Biosciences, Lincoln, NE, USA), goat-anti-rabbit-800 (Invitrogen), HRP goat-anti-mouse (Santa Cruz Biotechnology) and

HRP-goat-anti-rabbit (Bio-Rad, Hamburg, Germany). For detection the enhanced chemiluminescence system (GE Healthcare) or the Odyssey infrared imaging system (LI-COR biosciences) was used.

Immunostaining and confocal microscopy. Cells were seeded in ibidi- μ -slides (ibidi), treated as indicated, washed, fixed with 4% paraformaldehyde, permeabilized with 1% Triton-X 100 and incubated with 1% bovine serum albumin solution to block unspecific binding of antibodies. The following primary antibodies were incubated overnight at 4°C: PKC α , PKC ϵ (Santa Cruz Biotechnology) and Hexokinase II (Cell Signaling Technology). Goat-anti-rabbit-Alexa647 antibody (Invitrogen) was used as secondary antibody and incubated with 0.5 μ g/ml Hoechst 33342 (Sigma-Aldrich) for 2 h. Mitochondrial staining was achieved by using MitoTracker Red CMXRos (Invitrogen) according to the manufacturer's instructions. Stainings were visualized using the confocal microscope LSM 510 Meta (Zeiss).

Cell fractionations. For cytosolic-mitochondrial fractionation, mitochondrial fractions were prepared as previously described.⁴⁴ In brief, cells were harvested and lysed with a buffer containing digitonin (80 μ g/ml) and centrifuged at 500 \times g to remove cell debris. Supernatants were collected and centrifuged at 12 000 \times g to separate the mitochondrial fraction from the cytosolic one. The pellet containing the mitochondrial fraction was washed with ice-cold PBS and permeabilized using 0.1% Triton-X 100. For functional analysis, mitochondria were isolated as described previously.⁴⁵ Protein content was determined via Bradford and equal amounts of protein were separated using SDS-PAGE.

For cytosolic-cytoskeletal fractionation, cytoskeletal preparation was modified from Zeidman *et al.*⁵ Briefly, cells were lysed for 20 min on ice with the lysis buffer mentioned in the western blot section. Lysates were centrifuged at 500 \times g for 10 min to remove nuclei and cell debris. Supernatants containing cytosolic and cytoskeletal proteins were centrifuged at 12 000 \times g for 15 min to separate CSK. Proteins of supernatant and CSK pellet were separated using SDS-PAGE and blotted on nitrocellulose membrane (GE Healthcare).

Overexpression of PKC ϵ . FLAG.PKCepsilon plasmid was a gift of Alex Toker⁴⁶ (Addgene plasmid 10795). MCF7 cells were transfected using the Amara Nucleofector kit V (Lonza) according to the manufacturer's instructions. MDA-MB-231 cells were transfected using FuGene HD transfection kit (Promega). pcDNA3.1 (Invitrogen) was used as empty vector control. Upregulation of PKC ϵ was confirmed on protein level via western blot. At 24 h after transfection, cells were treated with ChA at indicated concentrations.

Downregulation of PKC ϵ . MDA-MB-231 cells were transfected for 72 h using Dharmafect transfection reagent (GE Healthcare, Buckinghamshire, UK) according to the manufacturer's instructions. The siRNA used for the experiments was ON-TARGETplus PRKCE siRNA from Dharmacon (GE Healthcare).

Staining of mammary tissue sections. Tumor and healthy breast tissues were fixed in formalin and embedded in paraffin blocks. Sections were stained with anti-PKC ϵ antibody (Abcam, San Francisco, CA, USA) and visualized with the Vectastain ABC Kit (Vector Laboratories, Burlingame, CA, USA) according to the manufacturer's instructions. Four control tissues and six tumor tissues were analyzed and images were taken on an Olympus BX41 microscope (Olympus, Center Valley, PA, USA) with a 20-fold magnification.

In vivo mouse xenograft model. For the subcutaneous xenograft model, 5 \times 10⁶ MDA-MB-231 cells in Matrigel/PBS (1:1) were injected subcutaneously in

Figure 6 Chondramide affects tumor growth *in vivo* via actin polymerization-induced abrogation of PKC ϵ signaling. (a) Tumor volume of female SCID mice harboring a MDA-MB-231 tumor in their flank that were either treated with solvent control (DMSO) or 0.75 mg/kg/day Chondramide. Significance analysis was performed using Student's *t*-test with **P* < 0.05, ***P* < 0.01. (b) Statistical analysis of TUNEL-stained paraffin sections. Six fields per tumor were visualized and counted. (c) Cryosections of tumors were stained for actin (red), PKC ϵ (green) and nuclei (blue). Scale bar indicates 50 μ m. Representative images of a control and Chondramide-treated tumor borders are shown. Inserts in the merged images show a magnification of a few single cells. Bars represent the mean \pm S.E.M. of three independent experiments performed in triplicates, **P* < 0.05 (one-way ANOVA, Bonferroni). (d) Cartoon illustrating the mode of action of ChA. Physiological state: PKC ϵ activity leads to stabilization of the Hexokinase II/VDAC interaction and phosphorylation of Bad, both of which prevent efflux of cytochrome C and support survival of cancer cells. Chondramide A treatment: ChA leads to actin hyperpolymerization and impairment of PKC ϵ signaling, thereby to destabilization of the Hexokinase II/VDAC complex and dephosphorylation of Bad, resulting in cytochrome C release and induction of apoptosis

the flank of female SCID (C.B-17/lcrHanHsd-Prkdcscid, Harlan, Tampa, FL, USA) mice. At 9 days after tumor cell injection, 0.75 mg chondramide/kg in PBS/5% Solutol (BASF, Ludwigshafen, Germany) was injected intraperitoneally three times a week. After 34 days, mice were killed and tumor growth and tumor weight of control ($n = 10$) and Chondramide-treated mice ($n = 10$) was determined. Tumor volume was calculated every second day according to the formula $V = a \times b^2/2$ ($a =$ largest side of the tumor and $b =$ the largest side vertical to a). Average tumor volumes of the two groups were compared over time. Tumor tissues were either frozen in liquid nitrogen or fixed in formalin. Cryosections were stained for actin with rhodamine phalloidin (Invitrogen) and anti-PKC ϵ -antibody (Abcam) followed by incubation with anti-rabbit secondary antibody conjugated with Alexa 488 (Invitrogen). Formalin preserved sections were embedded in paraffin and stained for apoptotic cells by ApopTag Fluorescein In Situ Apoptosis Detection Kit (Merck Millipore) according to the manufacturer's instructions. TUNEL-positive cells were visualized with a Zeiss confocal microscope. Six randomly chosen images of each tumor were counted for TUNEL-positive nuclei. All animal procedures were approved and controlled by the local ethics committee and carried out according to the guidelines of the German law of protection of animal life.

Statistics. Statistical analysis was performed using the GraphPad Prism 5.0 software (La Jolla, CA, USA). Error bars indicate \pm S.E.M. One-way ANOVA with Bonferroni post-test or Student's t -test was used as significance analysis. A P -value of <0.05 was considered statistically significant.

Conflict of Interest

The authors declare no conflict of interest.

Acknowledgements. We thank Professor Dr. Stefan Zahler for his support of confocal microscopic imaging. Furthermore, Kerstin Loske and Sylvia Schnegg are acknowledged for their technical support. This research was supported by the Deutsche Forschungsgemeinschaft (DFG; FOR1406).

Author contributions

FF, SB and AMV designed the experiments; FF and CM performed the experiments; ES and DM provided human tumor sections; EW, JB and RK provided and performed the animal experiments; SH and RM isolated Chondramide; HZ and SS analyzed the data of isolated mitochondria assays; FF, SB and AMV wrote the manuscript.

- Franklin-Tong VE, Gourlay CW. A role for actin in regulating apoptosis/programmed cell death: evidence spanning yeast, plants and animals. *Biochem J* 2008; **413**: 389–404.
- Steinberg SF. Structural basis of protein kinase C isoform function. *Physiol Rev* 2008; **88**: 1341–1378.
- Prekeris R, Hernandez RM, Mayhew MW, White MK, Terrian DM. Molecular analysis of the interactions between protein kinase C-epsilon and filamentous actin. *J Biol Chem* 1998; **273**: 26790–26798.
- Baines CP, Song CX, Zheng YT, Wang GW, Zhang J, Wang OL *et al*. Protein kinase Cepsilon interacts with and inhibits the permeability transition pore in cardiac mitochondria. *Circ Res* 2003; **92**: 873–880.
- Zeidman R, Troller U, Raghunath A, Pahlman S, Larsson C. Protein kinase Cepsilon actin-binding site is important for neurite outgrowth during neuronal differentiation. *Mol Biol Cell* 2002; **13**: 12–24.
- Pan Q, Bao LW, Kleer CG, Sabel MS, Griffith KA, Teknos TN *et al*. Protein kinase C epsilon is a predictive biomarker of aggressive breast cancer and a validated target for RNA interference anticancer therapy. *Cancer Res* 2005; **65**: 8366–8371.
- Song MS, Park YK, Lee JH, Park K. Induction of glucose-regulated protein 78 by chronic hypoxia in human gastric tumor cells through a protein kinase C-epsilon/ERK/AP-1 signaling cascade. *Cancer Res* 2001; **61**: 8322–8330.
- Okhrimenko H, Lu W, Xiang C, Hamburger N, Kazimirovsky G, Brodie C. Protein kinase C-epsilon regulates the apoptosis and survival of glioma cells. *Cancer Res* 2005; **65**: 7301–7309.
- Toton E, Ignatowicz E, Skrzeczkowska K, Rybczynska M. Protein kinase Cepsilon as a cancer marker and target for anticancer therapy. *Pharmacol Rep* 2011; **63**: 19–29.
- Basu A, Sivaprasad U. Protein kinase Cepsilon makes the life and death decision. *Cell Signal* 2007; **19**: 1633–1642.
- Garg R, Blando J, Perez CJ, Wang H, Benavides FJ, Kazanietz MG. Activation of nuclear factor kappaB (NF-kappaB) in prostate cancer is mediated by protein kinase C epsilon (PKCepsilon). *J Biol Chem* 2012; **287**: 37570–37582.
- Newton PM, Messing RO. The substrates and binding partners of protein kinase Cepsilon. *Biochem J* 2010; **427**: 189–196.
- Daniel NN. BAD: undertaker by night, candyman by day. *Oncogene* 2008; **27**(Suppl 1): S53–S70.
- Galluzzi L, Kepp O, Tajeddine N, Kroemer G. Disruption of the hexokinase-VDAC complex for tumor therapy. *Oncogene* 2008; **27**: 4633–4635.
- Mathupala SP, Ko YH, Pedersen PL. Hexokinase II: cancer's double-edged sword acting as both facilitator and gatekeeper of malignancy when bound to mitochondria. *Oncogene* 2006; **25**: 4777–4786.
- McCommis KS, Baines CP. The role of VDAC in cell death: friend or foe? *Biochim Biophys Acta* 2012; **1818**: 1444–1450.
- Roy SS, Madesh M, Davies E, Antonsson B, Daniel N, Hajnoczky G. Bad targets the permeability transition pore independent of Bax or Bak to switch between Ca²⁺-dependent cell survival and death. *Mol Cell* 2009; **33**: 377–388.
- Kroemer G, Galluzzi L, Brenner C. Mitochondrial membrane permeabilization in cell death. *Physiol Rev* 2007; **87**: 99–163.
- Green DR, Kroemer G. The pathophysiology of mitochondrial cell death. *Science* 2004; **305**: 626–629.
- Bernardi P, Krauskopf A, Basso E, Petronilli V, Blachly-Dyson E, Di Lisa F *et al*. The mitochondrial permeability transition from in vitro artifact to disease target. *FEBS J* 2006; **273**: 2077–2099.
- Halestrap AP. A pore way to die: the role of mitochondria in reperfusion injury and cardioprotection. *Biochem Soc Trans* 2010; **38**: 841–860.
- Vander Heiden MG, Chandel NS, Williamson EK, Schumacker PT, Thompson CB. Bcl-xL regulates the membrane potential and volume homeostasis of mitochondria. *Cell* 1997; **91**: 627–637.
- Brenner C, Grimm S. The permeability transition pore complex in cancer cell death. *Oncogene* 2006; **25**: 4744–4756.
- Reubold TF, Eschenburg S. A molecular view on signal transduction by the apoptosome. *Cell Signal* 2012; **24**: 1420–1425.
- Crompton M, Ellinger H, Costi A. Inhibition by cyclosporin A of a Ca²⁺-dependent pore in heart mitochondria activated by inorganic phosphate and oxidative stress. *Biochem J* 1988; **255**: 357–360.
- Broekemeier KM, Dempsey ME, Pfeiffer DR. Cyclosporin A is a potent inhibitor of the inner membrane permeability transition in liver mitochondria. *J Biol Chem* 1989; **264**: 7826–7830.
- Sasse F, Kunze B, Gronewold TM, Reichenbach H. The chondramides: cytostatic agents from myxobacteria acting on the actin cytoskeleton. *J Natl Cancer Inst* 1998; **90**: 1559–1563.
- Eggert U, Diestel R, Sasse F, Jansen R, Kunze B, Kalesse M. Chondramide C: synthesis, configurational assignment, and structure-activity relationship studies. *Angew Chem Int Ed Engl* 2008; **47**: 6478–6482.
- Herrmann J, Huttel S, Muller R. Discovery and biological activity of new Chondramides from *Chondromyces* sp. *Chembiochem* 2013; **14**: 1573–1580.
- Hall A. The cytoskeleton and cancer. *Cancer Metastasis Rev* 2009; **28**: 5–14.
- Kuppens IE. Current state of the art of new tubulin inhibitors in the clinic. *Curr Clin Pharmacol* 2006; **1**: 57–70.
- Posey SC, Martelli MP, Azuma T, Kwiatkowski DJ, Bierer BE. Failure of gelsolin overexpression to regulate lymphocyte apoptosis. *Blood* 2000; **95**: 3483–3488.
- Bubb MR, Spector I, Beyer BB, Fosen KM. Effects of jasplakinolide on the kinetics of actin polymerization. An explanation for certain in vivo observations. *J Biol Chem* 2000; **275**: 5163–5170.
- Lazaro-Dieguez F, Aguado C, Mato E, Sanchez-Ruiz Y, Esteban I, Alberch J *et al*. Dynamics of an F-actin aggregate generated by the actin-stabilizing toxin jasplakinolide. *J Cell Sci* 2008; **121**: 1415–1425.
- Mochly-Rosen D, Das K, Grimes KV. Protein kinase C, an elusive therapeutic target? *Nat Rev Drug Discov* 2012; **11**: 937–957.
- Oliva JL, Caino MC, Senderowicz AM, Kazanietz MG. S-Phase-specific activation of PKC alpha induces senescence in non-small cell lung cancer cells. *J Biol Chem* 2008; **283**: 5466–5476.
- Lau E, Kluger H, Varsano T, Lee K, Scheffler I, Rimm DL *et al*. PKCepsilon promotes oncogenic functions of ATF2 in the nucleus while blocking its apoptotic function at mitochondria. *Cell* 2012; **148**: 543–555.
- Aziz MH, Manoharan HT, Church DR, Dreckschmidt NE, Zhong W, Oberley TD *et al*. Protein kinase Cepsilon interacts with signal transducers and activators of transcription 3 (Stat3), phosphorylates Stat3Ser727, and regulates its constitutive activation in prostate cancer. *Cancer Res* 2007; **67**: 8828–8838.
- Chiang CW, Kanies C, Kim KW, Fang WB, Parkhurst C, Xie M *et al*. Protein phosphatase 2A dephosphorylation of phosphoserine 112 plays the gatekeeper role for BAD-mediated apoptosis. *Mol Cell Biol* 2003; **23**: 6350–6362.
- Meshki J, Caino MC, von Burstin VA, Griner E, Kazanietz MG. Regulation of prostate cancer cell survival by protein kinase Cepsilon involves bad phosphorylation

- and modulation of the TNF α /JNK pathway. *J Biol Chem* 2010; **285**: 26033–26040.
41. Murakoshi H, Lee SJ, Yasuda R. Highly sensitive and quantitative FRET-FLIM imaging in single dendritic spines using improved non-radiative YFP. *Brain Cell Biol* 2008; **36**: 31–42.
42. Zamzami N, Metivier D, Kroemer G. Quantitation of mitochondrial transmembrane potential in cells and in isolated mitochondria. *Methods Enzymol* 2000; **322**: 208–213.
43. von Schwarzenberg K, Wiedmann RM, Oak P, Schulz S, Zischka H, Wanner G *et al*. Mode of cell death induction by pharmacological vacuolar H⁺-ATPase (V-ATPase) inhibition. *J Biol Chem* 2013; **288**: 1385–1396.
44. Rudy A, Lopez-Anton N, Barth N, Pettit GR, Dirsch VM, Schulze-Osthoff K *et al*. Role of Smac in cephalostatin-induced cell death. *Cell Death Differ* 2008; **15**: 1930–1940.
45. Schmitt S, Saathoff F, Meissner L, Schropp EM, Lichtmannegger J, Schulz S *et al*. A semi-automated method for isolating functionally intact mitochondria from cultured cells and tissue biopsies. *Anal Biochem* 2013; **443**: 66–74.
46. Cenni V, Doppler H, Sonnenburg ED, Maraldi N, Newton AC, Toker A. Regulation of novel protein kinase C epsilon by phosphorylation. *Biochem J* 2002; **363**: 537–545.



Cell Death and Disease is an open-access journal published by **Nature Publishing Group**. This work is licensed under a **Creative Commons Attribution-NonCommercial-ShareAlike 3.0 Unported License**. The images or other third party material in this article are included in the article's Creative Commons license, unless indicated otherwise in the credit line; if the material is not included under the Creative Commons license, users will need to obtain permission from the license holder to reproduce the material. To view a copy of this license, visit <http://creativecommons.org/licenses/by-nc-sa/3.0/>

Supplementary Information accompanies this paper on Cell Death and Disease website (<http://www.nature.com/cddis>)